

# Study on the chemical deposition on steel of zinc phosphate with other metallic cations and hexamethylen tetramine. I. Preparation and structural and chemical characterization

A. V. SANDU, C. CODDET<sup>a</sup>, C. BEJINARIU\*

*“Gheorghe Asachi” Technical University of Iasi, Faculty of Material Science and Engineering, Iasi, Romania*

*<sup>a</sup>LERMPS, Université de Technologie de Belfort-Montbéliard, 90010 Belfort Cedex, France*

The paper presents the influence of an surface agent (hexamethylenetetramine) of the insertion with Mg(II) and Ni(II) of the zinc phosphate layer on steel plates. The morphology, composition and the structure of the deposited layers by chemical precipitation has been characterized by SEM-EDX, XRD and 3D optical profilometry. The experimental data evidences the purpose of the surface agent and the two cations on the uniformity and compactness of the phosphate layers.

(Received May 9, 2012; accepted July 19, 2012)

*Keywords:* Zinc phosphates, Anticorrosion, SEM-EDX, XRD, 3D Profilometry

## 1. Introduction

The low soluble phosphate layers deposited on iron objects, next to the anti-corrosive/climatic protection (chemical, electrochemical and biological), can be used simultaneously in other applications, speculating a series of multiple complementary and competitive functions. One of them is increasing the mechanical resistance, with two aspects: abrasion resistance with compact, uniform and adequate plasticity structures or with bearing capacity for lubricant films, both involved subsequently to plastic processing. Second it can be used as support for paints, offering a good adherence, sometimes even better than primers or sealants [1-4].

In general, the passivant deposition on iron objects by chemical precipitation of orthophosphate of Zn(II) and Fe(II), even in the presence of leveling agents or surface additives, lead to the formation of micro-crystallites with 3D dendritic structures, with some cavities and discontinuities to the substrates, which decrease the reliability [5-7].

In order to obtain continuous layers, in the case of competitive precipitation, is necessary to involve compatible metallic cations and reaction mediums that generate compact, uniform and adherent structures to the substrate [8-15].

The literature abound in phosphate recipes, each more complex, involving cations from “P” block, but also from “D” and “F” [16-20].

It is known that the phosphate ion with a slightly deformed tetrahedral structure is susceptible to form (in aqueous and acid mediums) low soluble salts (simple and double) [1-4].

When the precipitation solutions contain two or more divalent cations from “P” and “D” groups they are in competitiveness of precipitation, obtained by the compatibility in forming the 3D structures and the stratified ones with ortho- and meta-phosphate anions [1-4].

The chemical composition and the crystallographic structure of this layer depend on the compositions of the substrate and the phosphating bath. Two of the common phosphate structures are  $Zn_3(PO_4)_2 \cdot 4H_2O$  (hopeite) and  $Zn_2Fe(PO_4)_2 \cdot 4H_2O$  (phosphophyllite) [1-4, 8-14].

Zn phosphating is one of the most widely used treatments and is generally conducted in acid aqueous phosphate solutions containing zinc ions and phosphoric acid, as well as nitrate ions as accelerator to promote the oxidation and dissolution of the metallic surface [13]. It is known that the phosphate coating develops via the nucleation, growth, and coalescence of Zn phosphate grains. The corrosion resistance of the phosphate coating is related to the size and population density of pores in the coating [13]; that is, the pores provide a path for corrosion attack [14, 15].

The paper presents the obtaining of new zinc phosphate layer on iron surfaces. The layers were structural and chemical investigated by the use of SEM-EDX, optical 3D profilometry and XRD.

## 2. Materials and methods

The sample plates used are steel DC 01 type, according to US standards: Carbon Steel **AISI 1010** (SR EN 10130), used for plastic processing. The samples are round with the diameter of 20 mm.

The researches have been carried out with a SEM VEGA II LSH scanning electron microscope manufactured by the TESCAN Co., the Czech Republic, coupled with an EDX QUANTAX QX2 detector manufactured by the BRUKER/ROENTEC Co., Germany.

The topographical surface analysis was done with an optical 3D Profilometer AltiSurf 500 by AltiMet.

For obtaining the X-ray diffractograms and Brucker XRD was involved.

### 3. Layer deposition

The processes begin with degreasing in mild alkaline bath (10 min) followed by pickling in an acid solution (30 min) and then immersion in the phosphate bath of the steel samples. We started from an initial phosphate solution, containing 8.0 mL  $H_3PO_4$  98%, Zn 4.0g, 3.0 mL  $HNO_3$  60%, 0.8g NaOH, 0.5g  $NaNO_2$ , 0.03g  $Na_3P_3O_{10}$  for one liter of solution. In this solution sample named P1 was obtained.

By adding to the initial solution 12g  $Ni(NO_3)_2 \cdot 6H_2O$  per liter sample P2 and by adding 15g  $Mg(NO_3)_2 \cdot 6H_2O$  sample P3. Sample P4 was merged in initial solution with a content of 2 g hexamethylene tetramine.

All the samples were merged for 30 mins in the phosphate solutions at 90°C.

### 4. Results and discussions

In Fig. 1 we can observe that the deposited layers have dendritic structures with different morphology for all four obtaining procedures.

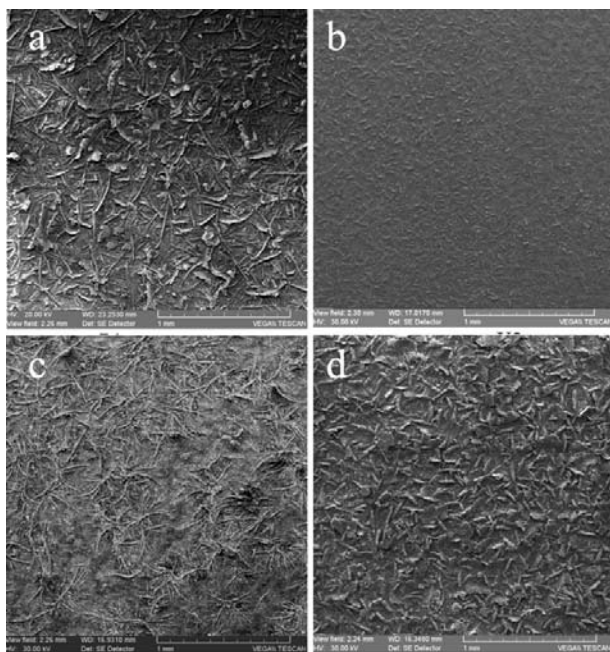


Fig. 1. SEM Images of the samples at 100X SE (scale bar = 1 mm): a – P1; b – P2; c – P3; d – P4

Thus for thin layers of ortho-phosphates of Zn(II) and Fe(II), obtained by coprecipitation in aqueous solution with orthophosphoric and nitric acid, involving competitive processes of substitution and addition [16-22], a non-uniform rough structure with long/flatt ramified crystallites are formed (Fig. 1A). The layers with Ni(II) present a very fine structure which is compact and uniform (Fig. 1B). In presence of Mg(II) dendritic cluster structures with long and thin micro-crystallites are obtained on a continuous flat film (Fig. 1C). In the presence of surface agents these are decreasing the lengths but getting thicker, becoming more compact with more flat structures (Fig. 1D).

According to the EDX data from table 1, evaluated on the surfaces shown in Fig. 1, we can observe that the molar ration (Fe+Zn+Mg+Ni):P vary like this:

$$P2 (2,62) < P4 (2,90) < P3 (4,55) < P1 (5,24)$$

this being very well corelated to the compactness of the layers shown in Fig. 1.

Table 1. EDX surface analysis results (atomic percents).

Sample/Element	P1	P2	P3	P4
Iron	34.23	23.33	39.31	18.67
Zinc	13.11	9.56	6.88	14.16
Phosphorus	9.03	12.71	8.95	11.22
Nickel	-	0.49	-	-
Magnesium	-	-	0.55	-
Nitrogen	-	-	2.11	1.99
Oxygen	43.63	53.91	42.20	53.96

For sample P2 and P3 we can observe that zinc is substituted by nickel and respectively magnesium and for sample P4 the concentration of zinc is higher in the detriment of iron, because of the surface agent that passivates the iron substrate.

In all four samples the O:P ratio is approximately 4, which corresponds with stoichiometric ratio of the ortho-phosphate, the oxygen excess being attributed to pyro bonds and the water from crystal hydrates.

In Fig. 2 are presented the X-ray spectrums which evidentiate the presence of congruent structures as phosphophyllite -  $Zn_2Fe(PO_4)_2 \cdot 4H_2O$ , nickel metaphosphate -  $Ni(PO_3)_2$  and zinc magnesium orthophosphate -  $Zn_2Mg(PO_4)_2$ . Note that phosphophyllite is present in all structures.

Also, this data can justify the value over 4 of the O:P ratio from Table 1. The presence of nickel as metaphosphate, structurally compatible with the ortho-phosphates, allows the formation of thin phosphate ceramic layers, climatic and mechanic resistant.

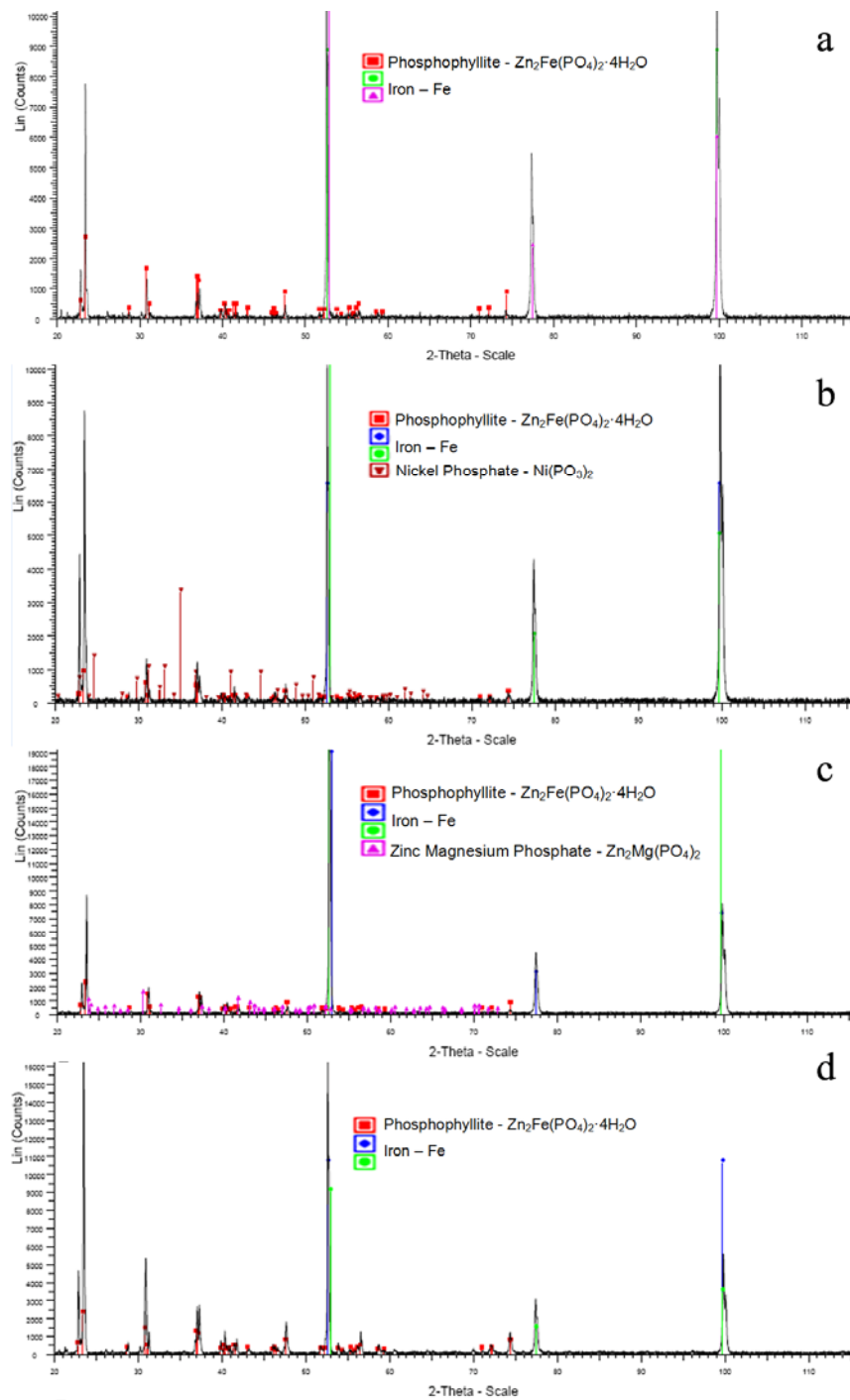


Fig. 2. XRD Spectrums of the samples from 20 to 120°:  
 a – P1, b – P2, c – P3, d – P4.

The data concerning the roughness obtained with the 3D optical profilometer (table 2 and figure 3) evidentiates that sample P4 has a rough structure with highest tickness and P2 is the finest structure. Roughness was obtained as average on multiple tests ( $n = 8$ ) on a 5,6 mm line.

Table 2. The roughness of the samples.

Sample	P1	P2	P3	P4
Ra ( $\mu\text{m}$ )	1,48	1,20	1,64	5,65

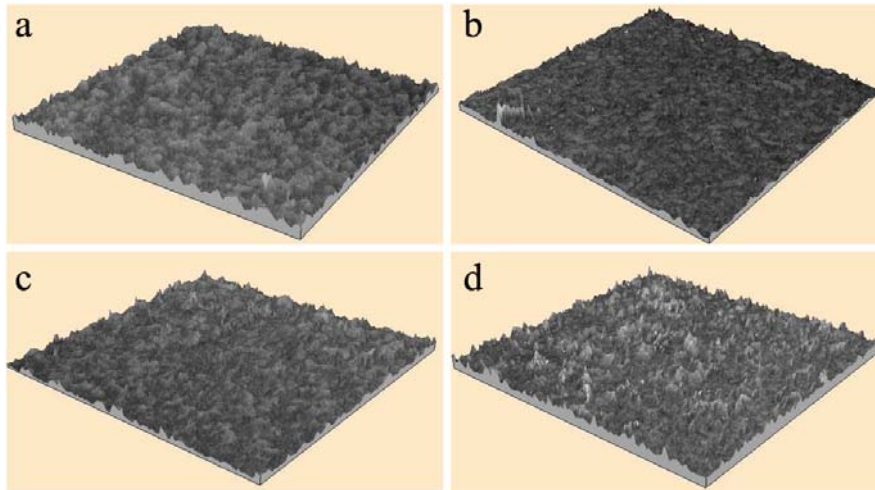


Fig. 3. 3D profiles of the sample's surfaces:  
a – P1, b – P2, c – P3, d – P4

After analyzing the distribution of the particle size on surface unit (Fig. 4.) we observe that sample P2 is the most homogenous. The samples have different distribution curves, having the maximum amplitudes for P1 at 11 microns, P2 at 12 microns, P3 at 13 microns and P4 at 35

microns, and the diameter of particles vary for P1 from 3 to 18 microns, for P2 from 4 to 26 microns, for P3 from 6 to 26 microns and for P4 from 20 to 70 microns. This is correlated to the photogrammetric data from the SEM images.

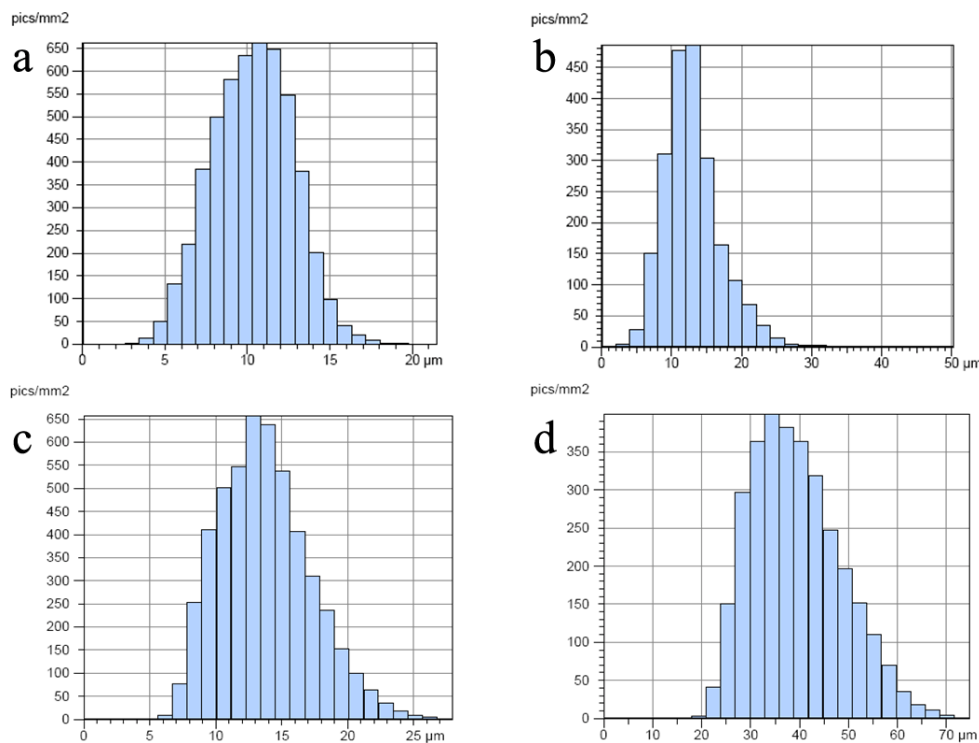


Fig. 4 The particle size distribution on surface: a – P1, b – P2, c – P3, d – P4

## 5. Conclusions

From the study of the chemical and physical-structural characteristics with SEM-EDX, XRD and optical

profilometry of the four passive phosphate layers, we conclude that:

- the ortho-phosphate layer of Zn(II) și Fe(II) obtained by coprecipitation in acid aqueous solution is influenced by the presence of other cations and anions and

active surface agents, which dictate the morphology and distribution of low soluble phosphates crystallites.

- The uniformity and compactness of the layer is dependent on the compatibility of the formed congruent structures, respectively the ortho- and meta-phosphate structures, anhydrous or hydrated.

- The molar ratio (Fe+Zn+Mg+Ni):P vary in the series P2 (2,62) < P4 (2,90) < P3 (4,55) < P1 (5,24), which is very well correlated with the compactness and uniformity of layers;

- Substitution of zinc with nickel and magnesium is obvious for samples P2 and P4, and in the case of P4 the iron is lower due to passive activity of the surface agent;

- The ratio O:P is aproximatively 4, for all the sample, corresponding with the stoichiometric ratio of the ortho-phosphate, the excess of the oxygen is due to pyro bonds and the water from cristal hydrates;

- The passive layer is formed from congruent structures like phosphophyllite -  $Zn_2Fe(PO_4)_2 \cdot 4H_2O$ , nickel metaphosphate -  $Ni(PO_3)_2$  and zinc magnesium phosphate -  $Zn_2Mg(PO_4)_2$ ;

- phosphophyllite is present in all the samples, which justifies the value over 4 of the O:P ratio;

- Nickel metaphosphate from P2, structural compatible with the ortho-phosphates, allows the formation of thin phosphate ceramic layers with high climatic and mechanic rezistivity;

- The activ surface agent (hexamethilen tetramine) allows the obtaining of rough and thick layers with large crystals;

- The granulometry distribution courves shows that P2 is the most homogen and compact layer with a fine structure.

### Aknowledgements

This paper was realized with the support of EURODOC "Doctoral Scholarships for research performance at European level" project, financed by the European Social Found and Romanian Government.

### References

- [1] A. Marinescu, Gh. Andoniant, E. Bay, Electrochemical and Chemical Technologies of Protection of Metallic Materials, Ed. Tehnica, Bucuresti, 1984.
- [2] H.E. Townsend, NACE Annual Corrosion Conference, Cincinnati, OH, paper 416, 1991.
- [3] L. Oniciu, E. Grüwald. Galvanotechnica, Ed. Științifică și Enciclopedică, Bucuresti, 1980.
- [4] W. Rausch, The Phosphating of Metals, Finishing Publications Ltd. (UK), 1990.
- [5] C. Bejinariu, I. Sandu, A. Predescu, I.G. Sandu, C. Baci, A.V. Sandu, Bulletin of the Polytechnic Institute of Iași, Section Material Science and Engineering, LV (LIX), **1**, 73 (2009).
- [6] A.V. Sandu, C. Bejinariu C., Bulletin of the Polytechnic Institute of Iași, Section Material Science and Engineering, Tom LVI (LX), **2**, 113 (2010).
- [7] A.V. Sandu, C. Bejinariu C., Bulletin of the Polytechnic Institute of Iași, Section Material Science and Engineering, Tom LVI (LX), **4**, 97 (2010).
- [8] J.M. Martin, Tribology Letters, **6**, 1 (1999).
- [9] F. Fang, J.H. Jiang, S.Y. Tan, A.B. Ma, J.Q. Jiang, Surface & Coatings Technology, **204**, 2381 (2010).
- [10] M. Sheng, Y. Wang, Q. Zhong, H. Wu, Q. Zhou, H. Lin, Surface & Coatings Technology, **205**, 3455 (2011).
- [11] B. Narayanasamy, A.J. Amalraj, J.A. Selvi, S. Rajendran, Bulletin of Electrochemistry, **21**, 489 (2005).
- [12] E.I. Ghali, R.J.A. Potvin, Corrosion Science, **12**, 583 (1972).
- [13] E.P. Banczek, P.R.P. Rodrigues, I. Costa, Surface and Coatings Technology, **203**, 1213 (2009).
- [14] J. Creus, H. Mazille, H. Idrissi, Surface and Coatings Technology, **130**, 224 (2000).
- [15] C.H.S.B. Teixeira, E.A. Alvarenga, W.L. Vasconcelos, V.F.C. Lins, Materials and corrosion - Werkstoffe und Korrosion, **62**, 853 (2011).
- [16] C. Bejinariu, I. Sandu, V. Vasilache, I.G. Sandu, M.G. Bejinariu, A.V. Sandu, M. Sohaciu, V. Vasilache, Patent RO125456-A2/2010-05-28.
- [17] C. Bejinariu, I. Sandu, C. Predescu, V. Vasilache, C. Munteanu, A.V. Sandu, V. Vasilache, I.G. Sandu, Patent RO125457-A2/2010-05-28.
- [18] J. F. Gu, Bingyan, J. Optoelectron. Adv. Mater. **10**, 405 (2008).
- [19] V.I. Trusov, V.L. Kiselev, Patent RU2241069 (C2)/2004.
- [20] N.V. Varentsova, V.A. Chumaevskij, Patent RU2111282 (C1)/1998.
- [21] A.V. Sandu, C. Coddet, C. Bejinariu, Revista de Chimie, **63**, 311 (2012).
- [22] A.V. Sandu, C. Bejinariu, A. Predescu, I.G. Sandu, C. Baci, I. Sandu, Recent Patents on Corrosion Science, **1**, 33 (2011).

\*Corresponding author: costica.bejinariu@yahoo.com